Author Manuscript

Author Manuscript

Author Manuscript

Author Manuscript

HHS Public Access

Author manuscript

Biophys J. Author manuscript; available in PMC 2026 May 08.

Published in final edited form as:

Biophys J. 2026 January 20; 125(2): 530–545. doi:10.1016/j.bpj.2025.08.030.

How regular are chromatin fiber topologies? The influence of $10n$ and $10n+5$ linker spacing explored by mesoscale modeling

Zilong Li[1], **Stephanie Portillo-Ledesma**[1], **Moshe Janani**[1], **Tamar Schlick**[1,2,3,4,*]

[1]Department of Chemistry, 100 Washington Square East, Silver Building, New York University, New York, NY 10003 U.S.A.

[2]Courant Institute of Mathematical Sciences, New York University, 251 Mercer St., New York, NY 10012 U.S.A.

[3]New York University-East China Normal University Center for Computational Chemistry, New York University Shanghai, Shanghai 200122 China.

[4]Simons Center for Computational Physical Chemistry, 24 Waverly Place, Silver Building, New York University, New York, NY 10003 U.S.A.

Abstract

The structural organization of chromatin is intricately influenced by the length of linker DNA connecting nucleosomes. Some studies have suggested that linker lengths tend to adopt $10n$ and $10n + 5$ base pairs values. Because these lengths dictate the rotational orientation of successive nucleosomes in the fiber axis, they can markedly affect chromatin fiber compaction and topology. Using a refined mesoscale chromatin model with 5 bp resolution, we investigated the influence of linker DNA periodicity, linker histone density, salt concentration, and starting fiber topology on chromatin architecture for regular fibers versus "life-like" fibers, the latter with irregular spacing between nucleosomes. Our results reveal that regular fibers with $10n$ linkers exhibit compact zigzag configurations, while $10n + 5$ linkers generate more open and flexible structures. However, these effects are pronounced only for short linker lengths, and longer linkers are more heterogeneous. Moreover, increased linker histone density further enhances compaction for long linker lengths, and lower salt concentration modifies chromatin topologies, diminishing periodicity-driven effects. In addition, periodicity effects are negligible in solenoid fibers, where tightly packed configurations override rotational influences. All these regular trends are reduced in life-like fibers with irregularly spaced nucleosomes despite having the same average spacing. Moreover, the trend details depend highly on specific features of the fiber architecture as designed

*Correspondence: schlick@nyu.edu.

AUTHOR CONTRIBUTIONS

Z.L. designed the research, performed data analysis, wrote the manuscript, prepared figures, and performed MC simulations. S.P.-L. designed the research, and wrote the manuscript. M.J. performed MC simulations. T.S. designed the research, reviewed the data and results analysis, wrote the manuscript, and obtained funding.

DECLARATION OF INTEREST

The authors declare no competing interests.

Publisher's Disclaimer: This is a PDF file of an unedited manuscript that has been accepted for publication. As a service to our customers we are providing this early version of the manuscript. The manuscript will undergo copyediting, typesetting, and review of the resulting proof before it is published in its final form. Please note that during the production process errors may be discovered which could affect the content, and all legal disclaimers that apply to the journal pertain.

Author Manuscript Author Manuscript Author Manuscript Author Manuscript

in experiments and simulations. Overall, our study highlights these detailed differences in models versus results and emphasizes the role of linker DNA length in regulating chromatin fiber architecture and its potential implications for genome accessibility and expression.

INTRODUCTION

In eukaryotes, the DNA wraps ~1.7 times (~147 bp) around octamers of histone proteins (two copies of H2A, H2B, H3, and H4) to form the nucleosome (1). The DNA connecting nucleosomes is termed linker DNA and its length varies widely, from ~10 to 100 bp (2), depending on cell type and state.

Many experimental studies in eukaryotes have suggested that rather than adopt a continuous range of values, the length of the linker DNA is preferentially quantized (3). Early studies on several eukaryotic cells (yeast, HeLa, chicken erythrocytes, and rat liver) showed that DNA fragments tend to have linker DNA with multiples of ~10 bp ($10n$, with n an integer) or also $10n + 5$ (4–8). More recent studies with higher precision in DNA cleavage and sequencing have supported the $10n + 5$ periodicity in yeast (9–12) and mouse (13). However, other periodicities have been identified, such as $10.6n + 8$ for Caenorhabditis elegans and Drosophila melanogaster (14), and $10n + 8$ for human k562 cells (15).

Each DNA base pair increases the distance between two consecutive nucleosomes by ~0.34 nm and is coupled to ~35° rotation about the DNA helix axis. A complete helical turn about the DNA axis occurs every 10.2–10.5 bp. Thus, linker DNAs with a $10n$ periodicity have an even number of DNA helical turns. That means that for a linker DNA of $10n$ bp, a nucleosome $k + 1$ is translated along the DNA by ~$3.4n$ nm, and rotated by n turns. If instead the linker DNA has a length of $10n + 5$ bp, the nucleosome $k + 1$ is translated along the DNA by ~$3.4n + 1.7$ nm, and rotated by $n + 1/2$ turns.

Much effort has been made to understand the biological relevance of quantized $10n$ and $10n + 5$ linker DNA, and how this is related to the regulation of chromatin architecture and gene expression, as summarized in Table 1. It is important to appreciate the many nuances involved in these experimental and simulation studies. Differences in setting up the fiber initial structures, the size of nucleosome arrays, and fiber conditions like salt concentration and LH density impact greatly the overall folding results. The studies summarized in Table 1 illustrate that while many groups have explored the effects of $10n$ versus $10n + 5$ linker spacing, their results vary depending on modeling frameworks, experimental setups, and interpretive focus.

In several simulation and experimental papers, Zhurkin and Grigoryev's groups (16–19) consistently report that $10n$ spacing yields compact, supercoiled fibers with strong stacking (change in the DNA linking number, $\Delta Lk \approx -1.5$), while $10n + 5$ spacing results in more relaxed, flexible structures ($\Delta Lk \approx -1.0$), supporting the concept of topological polymorphism linked to gene regulation. They also find that $10n$ spacing enhances compaction and supercoiling, but highlight distinct interaction patterns. Strong interactions between alternate nucleosomes, typical of 2-start topologies, emerge for $10n$ systems and

Author Manuscript Author Manuscript Author Manuscript Author Manuscript

high interactions between every third nucleosome, typical of 3-start organizations, are prevalent in $10n + 5$ fibers (20, 21).

In contrast, Olson's group (22–25) reports nuanced mechanical consequences when using DNA base-pair parameters to setup their fibers: while their mesoscale simulations confirm structural differences between $10n$ and $10n + 5$ fibers, they emphasize changes in nucleosomal DNA twist, polymer flexibility, and higher-order folding patterns. They observe that fiber architecture depends on both nucleosomal DNA twist and linker DNA length. Nucleosomes with overtwisted DNA condense the fiber when linkers are $10n$ in length, but open the fiber when linkers are in the family of $10n + 5$ linkers. The opposite effect occurs for undertwisted nucleosomal DNA; $10n + 5$ fibers are more compact than $10n$ fibers. Further, 3-start configurations emerge in the Olson group's models for fibers with undertwisted nucleosomal DNA and $10n$ linkers, whereas 2-start configurations emerge for $10n + 5$ linkers. When nucleosomal DNA is overtwisted instead, strong 2-start topologies emerge for $10n$ linkers but 3-start topologies emerge for $10n + 5$ linkers.

Meanwhile, van Noort's group (26), using base-pair resolution simulations and single-molecule data, highlights the sensitivity of stacking energy and stiffness to single-base changes, with $10n$ favoring compaction and $10n + 5$ inhibiting stacking. Similarly, base-pair resolution simulations of trinucleosomes from the Takada's group show different classes of fiber configurations that occur with a 10 bp periodicity (27). Structures with linkers of $10n$ bp have high compaction and zigzag stacking interactions, whereas intermediate structures are more diverse. That many experimentally solved structures of chromatin arrays correspond to $10n$ linkers (28–32) could also support homogeneous and stable zigzag structures for such systems, in contrast to more heterogeneous and unstable ensembles for other linker lengths.

These varying perspectives reflect complementary insights into how linker spacing impacts chromatin properties across different biological and physical scales.

Of course, in vivo, linker length is not generally regular, and "life-like" distributions are important in directing gene folding, as demonstrated for the HOXC gene (33). The motivation of our work is to determine how properties of uniform fibers differ from those of "life-like" fibers, and how common parameters like salt and linker histones affect fiber folding. Indeed, with our chromatin mesoscale model, we have also emphasized the effect of linker DNA length on fiber architecture, e.g., (2, 34, 35), showing that depending on the linker DNA length, a variety of topologies can result, including the 2-start zigzag, 1-start solenoid, and more irregular forms, that tend to form as linkers lengthen. In particular, we showed that life-like distributions are necessary for driving long-range interactions seen in contact maps (35) and a variety of polymorphic forms (36); these differ greatly from topologies of ideal regular fibers.

Our coarse-grained model for the linker DNA to date has employed a resolution of ~9 bp per bead, which makes it unsuited to capture effects related to the uneven number of helical turns in the linker DNA. To explore this effect of linker length on chromatin architecture and gene expression, we refine our linker DNA model to a 5 bp resolution and explore

Author Manuscript Author Manuscript Author Manuscript Author Manuscript

topologies for $10n$ and $10n + 5$ regular fibers while also considering other important factors such as salt concentration, linker histone density, and zigzag versus solenoid start topologies. Overall, our results show that the periodicity of linker DNA length significantly impacts the architecture of chromatin fibers, particularly in the zigzag topology and short linkers. Fibers with linker DNA lengths corresponding to $10n$ bp favor compact, stable configurations with enhanced nucleosome stacking, while $10n + 5$ linkers result in more open, flexible structures. However, these periodicity effects are prominent only in fibers with short linkers; they diminish as the linker length increases. In addition, the inclusion of other realistic factors like linker histones, varied salt concentrations, and heterogeneous linkers, diminish or eliminate any marked periodicity trends. Implications to life-like gene systems are discussed.

MATERIALS AND METHODS

Chromatin mesoscale model

Our chromatin mesoscale model (reviewed in (37, 38)) coarse grains chromatin elements at different levels of resolution (Figure 1). Nucleosome cores are treated as disks with 300 Debye-Huckel charges calculated using the nucleosome atomic crystal structure solved at 1.9 Å (PDB 1kx5) (39) and the DiSCO algorithm (40–42) to mimic the surrounding electrostatic potential and electric field. N-terminal histone tails of H2A, H2B, H3, and H4 and C-terminal tail of H2A are coarse grained as 5 residues per bead with a two-step procedure that first coarse grains each residue as one bead and then coarse grains 5 beads as one super bead (43). The charge of each super bead is the sum of the charges of the 5 residues that compose it. Similar to histone tails, linker histone (LH) is coarse grained as 5 residues per bead but the bead charges are calculated by the DiSCO algorithm (44). The coarse-grained model of the H1E LH isoform we use here contains 6 beads for the globular head (GH) and 22 beads for the C-terminal domain (CTD). The short N-terminal domain is not included (44). The GH is positioned symmetrically on the nucleosome dyad axis, in agreement with crystallographic and NMR-based studies. This positioning ensures contacts with the nucleosome core and stabilization of 10–20 bp of both entry and exit linker DNA. The CTD dynamically condenses and interacts with either one or both linker DNAs, depending on salt concentration and fiber context. The linker DNA connecting nucleosomes cores is modeled with a combined worm-like chain and bead model (45).

The total potential energy function of the model for the MC protocol is:

$$E_{TOT} = E_S + E_B + E_T + E_{tS} + E_{tB} + E_{lhS} + E_{lhB} + E_V + E_C, \quad (1)$$

and it is expressed in terms of **r**, the collective position vector of the system. The energy terms E_S, E_B, and E_T correspond to the stretching, bending, and twisting contributions of the linker DNA and nucleosome cores. The terms E_{tS} and E_{tB} denote the stretching and bending energies of the histone tails, while E_{lhS} and E_{lhB} refer to the same contributions for

Author Manuscript Author Manuscript Author Manuscript Author Manuscript

the linker histones. Finally, E_V accounts for excluded volume interactions—repulsive forces that prevent particle overlap—and E_C captures electrostatic interactions among all beads.

Because here we focus on the effect of linker DNA on fiber architecture, we next detail the linker DNA model and changes introduced to change its resolution from ~9 to 5 bp.

The entering and exiting linker DNA are attached to the nucleosome core using the 1kx5 nucleosome geometry, so that the linker/nucleosome center/linker angle is 108°. According to this model, the linker DNAs are positioned in the plane normal to the nucleosome plane. The length of the linker DNA in our mesoscale model is controlled by the number of beads between nucleosomes. The resolution of the linker DNA model is ~9 bp, defined by the unstretched equilibrium distance between beads, $l_0 = 3$ nm. The distance between DNA base pairs ($rise$) is 0.34 nm, so the number of base pairs in 3 nm is: $N_{bp} = \frac{l_0}{rise} = \frac{3.0}{0.34} = 8.8$.

To increase the resolution of the linker DNA model, the parameter $l_0 = 3$ is reduced to 1.7 nm, so $N_{bp} = 5$ bp. In general, for an n bp resolution, we modify l_0 by $n \times 0.34$.

Modifying the resolution of the DNA model (i.e., l_0), affects DNA stretching, bending, and twisting energy terms, as well as the electrostatic interactions between DNA beads, as follows.

Stretching: The stretching energy between two beads is based on Hooke's law, and given by:

$$E_{S_i} = \frac{h}{2}(l_i - l_0)^2, \tag{2}$$

where $h = \frac{100 k_b T}{l_0^2}$ is the stretching constant, k_b is the Boltzmann's constant, and T is the absolute temperature, l_i is the distance between two beads.

Bending: The bending energy is also based on the Hooke's law, which is given by:

$$E_{B_i} = \frac{g}{2}(\beta_i - \beta_0)^2, \tag{3}$$

where $g = \frac{per \times k_b T}{l_0}$ is the bending constant, per is the persistence length, β_i is the Euler angle, and β_0 the equilibrium angle ($\beta_0 = 0$ for straight DNA).

Twisting: The twisting energy is given by:

Author Manuscript Author Manuscript Author Manuscript Author Manuscript

$$E_{T_i} = \frac{s}{2l_0}(\alpha_i + \gamma_i - \phi_0)^2, \tag{4}$$

where $s = 3.0 \times 10^{-12}\ erg\ nm$ is the torsional rigidity constant of DNA as obtained from experiments (46), α and γ are the local Euler angles attached to each DNA bead in the chromatin chain (α is the rotation around the local z-axis, and γ is the orientation of the bend in the plane orthogonal to the tangent vector), and ϕ_0 is a twist deviation penalty term.

To justify the twisting due to DNA, ϕ_0 is calculated as follows: considering the average rise between B-DNA base pairs $Ri = 3.4$ Å, and average twist $Twi = 34.95^{\circ}$; let the number of beads between two nucleosomes be N_b, then:

$$\begin{aligned} N_{bp} &= \frac{(N_b + 1) \times l_0}{Ri} \\ N_t &= \frac{N_{bp}}{10.3} \\ Rot_{DNA} &= round(N_t) \\ Rot_{bp} &= \frac{Rot_{DNA} \times 360}{N_{bp}} \\ Twi_{DNA} &= Rot_{bp} - Twi \\ Twi_l &= N_{bp} \times Twi_{DNA} \\ \phi_0 &= \frac{Twi_l}{N_b + 1} \end{aligned} \tag{5}$$

where N_{bp} is the number of base pairs, N_t is the number of turns, Rot_{DNA} is the DNA rotation, Rot_{bp} is the rotation per base pair, Twi_{DNA} is the DNA twist, and Twi_l is the whole linker twist.

Electrostatics: The electrostatic energy is calculated using the Debye-Hückel screened electrostatic potential, which is given by:

$$U_{DH}(q_i, q_j, r_{i,j}) = \frac{q_i q_j}{4\pi\varepsilon_0 \varepsilon r_{i,j}} exp(-\kappa r_{i,j}), \tag{6}$$

where q_i, q_j are the charges on the two beads, $r_{i,j}$ the distance between the two beads, ε the dielectric constant, and κ the inverse Debye length.

Here the charge on the DNA beads $q_{DNA} = \nu l_0$ is calculated by multiplying the effective linear charge density ν to the equilibrium "bond length" l_0, where ν is obtained from (47) as a function of the monovalent salt concentration.

Author Manuscript Author Manuscript Author Manuscript Author Manuscript

Thus, changing the value of l_0 affects the values of the stretching constant, bending constant, twisting constant, twist deviation penalty term, and charges on DNA beads.

Starting structure topologies: zigzag and solenoid

Our mesoscale chromatin model can perform simulations with any start topologies including zigzag and solenoid chromatin topologies (Figure 1B). These conformations for initial structures are built with the following strategy:

Core position: The model arranges nucleosome cores in a helical path. The core positions are determined by:

Helix radius (R): Distance from the axis of the helix to the core positions.

Helix pitch (P): The vertical distance per turn of the helix.

Angle per core (γ): Angular increment between consecutive nucleosome cores.

For a nucleosome core i,

$$\begin{aligned} x_i &= R\ \cos\ \gamma_i, \\ y_i &= R\ \sin\ \gamma_i, \\ z_i &= z_{i-1} + \frac{P\Delta\gamma}{2\pi} \end{aligned} \tag{7}$$

Here, helix radius R is calculated based on the linker length, γ, and the radius of a typical nucleosome (see details in Figure 1C). Pitch, P, is 11 nm for both zigzag and solenoid fibers, and the angle per core γ is described below.

Core orientation: The core orientations are updated with sequential rotational transformations with three rotation matrices $R_x(\alpha)$, $R_y(\beta)$, and $R_z(\gamma)$ as follows:

$$R_x(\alpha) = \begin{bmatrix} 1 & 0 & 0 \\ 0 & \cos\ \alpha & \sin\ \alpha \\ 0 & -\sin\ \alpha & \cos\ \alpha \end{bmatrix}, R_y(\beta) = \begin{bmatrix} \cos\ \beta & 0 & -\sin\ \beta \\ 0 & 1 & 0 \\ \sin\ \beta & 0 & \cos\ \beta \end{bmatrix}, R_z(\gamma) = \begin{bmatrix} \cos\ \gamma & \sin\ \gamma & 0 \\ -\sin\ \gamma & \cos\ \gamma & 0 \\ 0 & 0 & 1 \end{bmatrix}.$$

The final orientation is $R = R_z(\gamma) \cdot R_y(\beta) \cdot R_x(\alpha)$

The choice of α, β, and γ is: $\alpha = \beta = 0$, and $\gamma = -60°$ and 205° for solenoid and zigzag fibers, respectively. This choice of α and β creates an initial structure where nucleosomes are perpendicular to the fiber axis. When $\gamma = -60$ (solenoid), it corresponds to 6 nucleosomes per helical turn (360/60=6). When $\gamma = 205° \approx 180°$ (zigzag), it creates an alternating arrangement, where nucleosomes are less tightly packed and arranged in a zigzag pattern.

Author Manuscript Author Manuscript Author Manuscript Author Manuscript

Irregular fibers

To simulate chromatin fibers with variable linker DNA lengths at 5 bp resolution, we generate sets of 50 discrete linker length values for each system.

To ensure controlled average linker lengths, we used a random integer sampling approach constrained within the specified range. For each desired target mean (e.g., 45 bp), we initialized a random vector of 50 integers uniformly sampled from the inclusive range [15, 90]. The average of this initial vector was then iteratively adjusted to match the target mean by incrementing or decrementing randomly selected values by ±5, ensuring that all values remained within the allowed range. This adjustment continued until the mean of the vector meets the target value.

Each finalized set of 50 values was used as a representative distribution of linker DNA lengths under the given average condition. These distributions were subsequently used to construct chromatin fiber models with realistic variability while controlling for global compaction levels dictated by the mean linker length.

Sampling

To sample the conformational space of each chromatin fiber we use our tailored Monte Carlo simulation protocol (42, 48). Global and local random moves are used to create energetically favorable chromatin conformations. In particular, a global pivot move is used to randomly select a nucleosome core or DNA linker bead, define an axis across the particle, and rotate the shortest end of the chromatin chain around this axis. Local rotation and translation moves are also applied to DNA linker beads or nucleosome cores to rotate or translate them around and along a random axis across them. Moves are accepted or rejected based on Metropolis energy criterion (49). For histone tails we use regrow moves (43) in which a tail is randomly selected to be regrown and then beads from one end are deleted and regrown at the opposite end using the Rosenbluth scheme (50). For linker histones, we sample the C-terminal domain beads with local translation moves in the same way we do for DNA linker beads and cores (44).

In this work, we use 80 million of Monte Carlo steps to sample the 16-nucleosome and 50-nucleosome fibers. For each system, we ran 100 copies that are started from different random seed number and a residual DNA twist value of −12°, 0°, or +12° to mimic natural variations (51).

Analysis

Sedimentation Coefficient: The sedimentation coefficient at each salt concentration is computed using the following expression:

$$S_{20,w} = ((S_1 - S_0)^*\rho + S_0)^*\left(1 + \frac{R_1}{N_C}\sum_i \sum_j \frac{1}{R_{ij}}\right), \quad (8)$$

Author Manuscript Author Manuscript Author Manuscript Author Manuscript

where $S_0 = 11.1S$ and $S_1 = 12S$ are the sedimentation coefficients of a mononucleosome without LH (52) and with LH (53), respectively, ρ is the LH density on the fiber, $R_1 = 5.5$ nm is the radius of a nucleosome, N_C is the number of nucleosomes in the chromatin fiber, and R_{ij} is the distance between the nucleosomes i and j.

Packing Ratio: To characterize chromatin compaction, we calculate the fiber packing ratio, defined as the number of nucleosomes per 11 nm of fiber length:

$$P_R = \frac{11 * N_C}{Fiber - length}, \quad (9)$$

where N_C is the total number of nucleosomes and the fiber length is calculated by defining the fiber axis with a cubic smoothing spline interpolation to the nucleosomes x, y, and z coordinates; see (54).

RESULTS

Compaction trends for $10n$ vs. $10n + 5$ fibers

As summarized in Table 1, previous modeling studies, that differ in model details and system setup, have focused on understanding the role of linker DNA length, or nucleosome rotational positioning, on fiber folding and compaction.

Here we use our chromatin mesoscale model with finer 5 bp resolution to further investigate the effect of $10n$ vs. $10n + 5$ linker DNA. For characterizing chromatin compaction, we measure the packing ratio and sedimentation coefficients, but use only packing ratio to analyze periodicity trends as this is a local compaction indicator, directly related to the nucleosome rotational positioning.

Our Monte Carlo simulations of uniform chromatin fibers with linker lengths ranging from 15 to 70 bp at NaCl 150 mM and started from ideal zigzag topologies indicate that $10n + 5$ linkers produce more open and disordered fibers, as shown in Figure 2A. When linker lengths are less than 40 bp, fibers with $10n + 5$ linker DNAs exhibit a more open structure (indicated by smaller packing ratio and sedimentation coefficients) than fibers with $10n$ linkers. Additionally, fibers with 20 and 30 bp linker DNAs form ladder-like structures with nucleosomes arranged in parallel to one another and perpendicular to the global fiber axis, whereas fibers with 15, 25, and 35 bp linker DNAs display disordered nucleosome orientations despite having largely straight linkers.

However, for longer linker lengths (45 to 70 bp), the fibers tend to adopt increasingly disordered conformations, in agreement with experimental observations (20, 55). This is due to increased flexibility of the nucleosomes with longer linkers as we have shown before (2), and this diminishes any topological influence of linker regularity.

Author Manuscript Author Manuscript Author Manuscript Author Manuscript

The core-core interactions for these systems in Figure 2B show that for short linker lengths (less than 25 bp), the dominant interaction peak occurs at $k \pm 1$, indicating ladder-like structures. For linker lengths between 25 and 70 bp, the interaction peaks shift to $k \pm 2$, indicative of the classic zigzag topology. Additionally, although $k \pm 2$ contacts are dominant, for linkers of 40 to 70 bp, $10n + 5$ fibers have higher $k \pm 3$ interactions than their corresponding $10n$ fibers (Figure 2B, right plot inset), in alignment with previous observations showing that a 5-bp difference can convert a mostly two-start topology into a three-start arrangement (19, 21, 24, 56).

Effect of linker histones on the topologies of $10n$ vs. $10n + 5$ linker fibers

Linker histones (LH) play an important role in compacting chromatin fibers by binding to the entry and exit points of nucleosomal DNA, stabilizing chromatin structure (57).

By introducing a LH density of 0.5 LH per nucleosome, we find in Figure 3 that $10n + 5$ fibers of up to 35 bp are again consistently less compact and more disordered compared to their corresponding Figure 3 that $10n$ chromatin fibers. When LH density increases to 1 LH per nucleosome, periodicity effects are further reduced to fibers of up to 25 bp linkers.

For linker lengths in the range of 15 to 30 bp, we observe that increasing LH density does not enhance chromatin compaction. This is because the close spacing of nucleosomes of these ladder-like fibers at short linker lengths is already at a threshold (58). LH creates steric hindrance and pushes nucleosomes slightly apart rather than compacting the fiber.

In contrast, for longer linker lengths (≥40 bp), the addition of LH leads to a significant increase in fiber compaction. This effect is particularly pronounced at the LH density of 1 LH per nucleosome, where the additional LH molecules stabilize nucleosome-nucleosome interactions and reduce the flexibility of the linker DNA. The longer linkers provide sufficient spatial separation to accommodate LH binding without inducing steric clashes, allowing LH to exert its compaction-promoting effects effectively.

Effect of salt concentration

Salt concentration plays a critical role in modulating chromatin structure by influencing the electrostatic interactions between nucleosomes and linker DNA (20, 43). At high salt concentrations, the effective charge neutralization of DNA promotes nucleosome stacking and fiber compaction, facilitating the formation of dense chromatin structures. Conversely, at low salt concentrations, reduced electrostatic screening destabilizes these interactions, leading to more open fibers with increased structural heterogeneity. Additionally, the effects of salt on chromatin structure can be more complicated if mixtures of salts are considered. For example, variation in the proportion of mixed monovalent salts alters the sedimentation coefficients of chromatin arrays (59), and the mixed salts needed to capture transcriptional activity in positioned nucleosome arrays differ from those used in standard physical experiments (25).

We compare the trends in Figure 2 for 150 mM NaCl to behavior at low ionic strength of 5 mM NaCl in Figure 4. Sedimentation coefficients are consistently lower than at

Author Manuscript Author Manuscript Author Manuscript Author Manuscript

150 mM NaCl, in agreement with previous experimental measurements for 12-nucleosome arrays (20). Interestingly, the periodicity compaction trends no longer exist; fibers become progressively less compact as the linker DNA length increases from 15 to 35 bp.

The lower ionic strength weakens the electrostatic screening between negatively charged DNA segments and produces more open and less ordered chromatin structures. Longer linker DNAs exacerbate this effect, producing more accordion-like topologies. While we have studied the effect of different NaCl concentrations, it remains to be seen how other electrolytes such as potassium, also prevalent in nature (60), or mixed salts affect fiber folding and periodicity trends. From our work on magnesium ions, impact on internucleosome interaction patterns are expected, for example, mixed $k \pm 1/k \pm 2$ interactions (61).

Solenoid fiber topologies for $10n$ and $10n + 5$ linker organizations

Solenoid fibers represent a distinct chromatin topology characterized by a tightly packed, helical arrangement of nucleosomes with approximately six nucleosomes per helical turn (Figure 1C). In contrast to the zigzag topology, which features a two-start helical arrangement with alternating nucleosome positioning and straight linkers (Figure 1B). Their prevalence in vivo is not clear, but zigzag topologies and hybrid zigzag/solenoid arrangements are likely typical *in vivo* (44, 61).

Here we examine the folding of regular $10n$ vs. $10n + 5$ solenoid fibers at a physiological salt concentration of 150 mM NaCl without linker histones for linker DNA lengths ranging from 15 to 70 bp. From the packing ratio and sedimentation analysis in Figure 5A, we see no periodic patterns. However, an interesting observation emerges at 40 bp linker length, where the packing ratio and sedimentation coefficient are higher than at 35 or 45 bp.

Further analysis of core-core interactions in Figure 5B provides additional insight. For linker lengths greater than 40 bp, the fibers with starting solenoid topologies transition into zigzag-like configurations, as evidenced by the appearance of interaction peaks at $k \pm 2$, which are characteristic of zigzag fibers. This structural shift explains the increased condensation observed at 40 bp linker length. For longer linker lengths, zigzag topologies are favored, resulting in greater nucleosome stacking and compaction. At linker lengths shorter than 40 bp, the solenoid topology remains a local equilibrium, with no evidence of periodicity or transition to zigzag structures.

Effect of irregular linker DNA lengths

While the above results were obtained for uniform fibers, linker DNAs *in vivo* are heterogeneous (13), and both short and long linkers can be simultaneously present in chromatin fibers, with variations of as much as 20 bp (62).

To study the effect of heterogeneous linkers on the fiber periodicity, we construct 50-nucleosome fiber arrays with irregular linker lengths that yield the same average linker DNA length as the regular fiber. Specifically, we combined various linker lengths to design irregular chromatin fiber such that the overall average linker length matches a target value. For example, we achieve an average linker length of 20 bp by using a combination of 15,

Author Manuscript Author Manuscript Author Manuscript Author Manuscript

20, and 25 bp linkers as detailed in Methods. As shown in Figure 6A, chromatin fibers with irregular linker DNA lengths do not exhibit periodicity patterns, even when the average linker lengths correspond to $10n$ or $10n + 5$. This more life-like distribution of linker lengths introduces heterogeneity and disrupts any regular alignments that can occur with regular $10n$ or $10n + 5$ linker lengths.

From the packing ratio (Figure 6A, left), we see that the uniform fibers are always more locally compact than the life-like fibers. This is because the nucleosomes in life-like fibers have more freedom to adjust geometries due to the variability of linker lengths. The sedimentation values in Figure 6A, right, show that with shorter linker lengths (< 35 bp), the life-like fiber is more globally compact due to the fibers folding into blobs compared with the ladder-like uniform fibers. However, for longer linker lengths (> 35 bp), the uniform fibers are more compact, similarly to the packing ratio trends.

These results, along with prior studies on life-like systems (35), highlight that irregular distributions of linker lengths prevent any rotational alignment of nucleosomes, and diminish periodic patterns. Irregular fibers are more disordered and lack the distinctive compactness or openness characteristic of $10n$ or $10n + 5$ fibers.

Clearly, variability in linker DNA lengths, including nucleosome free regions (NFRs), serve as factors to modulate chromatin flexibility and accessibility, allowing for diverse structural and functional states. Importantly, ideal geometries are clearly very sensitive to other relevant factors found *in vivo*, such as the salt concentration, LH density, epigenetic marks, and more, as we have shown in folding gene systems like HOXC (33), Pou5f1 (63) and others (64).

Effect of linker DNA resolution on chromatin fiber architecture: 5 vs. ~9 bp resolution

Our prior mesoscale chromatin model with ~9 bp resolution linker DNA beads has demonstrated its utility capturing essential features of chromatin architecture, particularly in systems with diverse and longer linker DNA lengths. As a self consistency check, here also compare the behavior of the ~9 bp resolution model vs. the new 5 bp model. For long linkers, behavior should be very similar, although for short linkers, we expect differences.

Figure 7 shows packing ratio and sedimentation trends as a function of linker DNA length. We see that both models, the ~9 bp and 5 bp resolution, produce aligned results as linker length increases. Clearly, periodicity for $10n$ and $10n + 5$ linker DNA lengths at very short linkers cannot be captured by the ~9 bp resolution model.

Computationally, however, the ~9 bp mesoscale model is far more efficient. Our Monte Carlo simulations of 16-nucleosome fibers using the ~9 bp resolution model converge in approximately 20 million steps, whereas the 5 bp resolution model requires 80 million steps to reach convergence. This increased computational cost for the finer model is due to the higher number of particles involved, as measured by equilibration of local and global measurements (65). Increasing the number of DNA beads also affects the calculation time and memory requirements; due to the nonbonded terms, the energy evaluation scales as

Author Manuscript Author Manuscript Author Manuscript Author Manuscript

$O(n^2)$, where n is the total number of beads (core, histone tails, linker DNA and linker histones).

As is well known, the choice of model should suit the biological problem being addressed. Hence for gene-level questions, such as in recent studies (64, 66, 67), a more efficient nucleosome resolution model is preferred, while for small fibers with short linker DNA, a finer resolution is important.

DISCUSSION

The compaction analysis of regular $10n$ vs. $10n + 5$ linker lengths fibers shows some periodic trends among very short linkers that are modulated by salt concentration, LH density, and chromatin start topology. However, as linker DNA length extends beyond 40 bp, periodicity effects are largely diminished. Overall, our results indicating that $10n + 5$ fibers are less compact and more disordered than their corresponding $10n$ fibers agree with some modeling (16, 17, 21, 27) and experimental (18, 20, 21) results. These results were obtained for zigzag starting models and considered undertwisted nucleosomes. On the other hand, higher compaction for $10n + 5$ has been obtained by another model that considers 3-start topologies and accounts for different nucleosomal DNA twisting (22, 24, 25). These differences naturally define future work to study the influence of these additional parameters.

In vivo, chromatin is highly heterogeneous, and truly uniform chromatin fibers are rare. Linker DNA lengths distributions are affected by developmental stage, cell type, and even disease state. As we see from Table 2 summarizing how linker length ranges for different organisms, the high variability of linker DNA lengths across species is evident, suggesting that chromatin is not uniformly organized in most biological contexts. However, in specific cases, like chicken erythrocytes (68) and mouse embryonic stem cells (13), relatively uniform linker lengths are found, where $10n$ and $10n + 5$ periodicity could play a functional role in stabilizing chromatin architecture. Similarly, in special cases like telomeres (69) and neurons in the cerebral cortex (70), the mammalian genome exhibits very short linker DNAs.

Our work also underscores how cellular environment such as the salt concentration and linker histone density can modulate or even override intrinsic fiber tendencies. In vivo, the nuclear ionic environment is dynamic and spatially heterogeneous, suggesting that chromatin periodicity and compaction may be locally regulated by ion fluxes or salt gradients. Thus, changes in the nuclear microenvironments contribute profoundly to mechanisms of gene regulation.

Our comparison between 5 bp and ~ 9 bp resolution models reveals a tradeoff between computational efficiency and physical accuracy. While the ~ 9 bp resolution is sufficient for capturing global compaction trends, the finer 5 bp resolution is necessary to resolve effects related to helical twist and internucleosomal orientation. Although the trend has been to develop coarse-grained models to capture large chromosome and chromosomal territory behavior, finer scales may be important for a mechanistic understanding of detailed topological transitions or experimental systems with known periodicity.

Author Manuscript Author Manuscript Author Manuscript Author Manuscript

Our demonstration that introducing irregularity into linker lengths—closer to *in vivo* conditions—eliminates the structural periodicity seen in uniform fibers supports a dynamic view of chromatin where flexibility and polymorphism are advantageous for biological function, allowing for diverse chromatin states. This agrees with recent imaging and modeling studies suggesting that heterogeneous fibers are necessary for forming long-range chromatin contacts observed in Hi-C maps (33, 72).

A key novelty of our work lies in the systematic inclusion of linker histones (LHs) and life-like irregular fiber models, two factors that have often been overlooked or simplified in prior studies of linker DNA periodicity. While most previous simulation efforts focused on uniform, ideal fibers without LHs, our study reveals how LH density modulates fiber compaction in a linker-length-dependent manner. Specifically, we show that LHs enhance compaction for long linker lengths (≥40 bp), but exert minimal or even disruptive effects at short linker lengths due to steric hindrance. This finding offers mechanistic insight into how LH binding may selectively stabilize longer-linker chromatin regions in vivo. In addition, we incorporate more biologically realistic fiber configurations by simulating life-like fibers with heterogeneous linker distributions centered at $10n$ or $10n + 5$ means. These irregular fibers show that even minor deviations from uniform spacing eliminate the clear periodicity trends observed in ideal fibers, underscoring the importance of linker heterogeneity in generating flexible, polymorphic chromatin ensembles. Furthermore, our use of a refined 5 bp resolution model enables us to resolve helical phasing and torsional effects associated with linker DNA geometry, bridging the gap between coarse mesoscale models and fine-grained DNA-level features. Together, these contributions provide a more nuanced and physiologically relevant view of how linker DNA periodicity and associated chromatin features influence fiber folding and genome organization.

Clearly, while our simulations begin from idealized zigzag or solenoid topologies; and are useful for identifying trends, they may not fully capture the stochastic and dynamic processes of chromatin folding in living cells. Future work can be extended to study heterogeneous fibers with biologically realistic distributions of nucleosome spacing, such as obtained from experimental MNase-seq or ATAC-seq data. Applications to explore how linker length periodicity may influence enhancer–promoter communication, the mechanical response of chromatin under torsional stress, and consideration of the variation in twisting of nucleosomal DNA, also define the intriguing direction for further work.

CONCLUSION

This study advances our understanding of how linker DNA periodicity in regular, ideal fibers and related factors regulate chromatin fiber architecture. Our findings demonstrate that $10n$ and $10n + 5$ periodicities influence chromatin compaction and topology only at very short linker lengths, with effects modulated by linker length, LH density, and salt concentration. Importantly, in life-like fibers containing a mixture of linker DNA lengths, periodicity effects are lost, even for short linkers.

Overall, the results provide valuable insights into chromatin organization, emphasizing the interplay between DNA geometry and environmental factors in genome regulation. Future

Author Manuscript Author Manuscript Author Manuscript Author Manuscript

studies could explore the implications of these findings for transcriptional regulation, DNA repair, and higher-order chromatin organization, further bridging the gap between chromatin structure and function.

Supplementary Material

Refer to Web version on PubMed Central for supplementary material.

ACKNOWLEDGMENTS

We thank Professor Wilma Olson for motivating this research and many insightful comments. We gratefully acknowledge support from the Simons Foundation through the NYU Simons Center for Computational Physical Chemistry. This work was supported in part through the NYU IT High Performance Computing (HPC) group, which provided resources, services, and expert advice. This work was supported by the National Institutes of Health, National Institutes of General Medical Sciences Award R35-GM122562, the National Science Foundation Awards 2151777 and 2330628 from the Division of Mathematical Sciences and Award 2337391 from the Molecular Cellular Biosciences Core Programs, and Philip-Morris International to T.S.

REFERENCES

1. Kornberg RD, 1974. Chromatin structure: A repeating unit of histones and DNA. Science 184:868–871. http://science.sciencemag.org/content/184/4139/868. [PubMed: 4825889]
2. Perišić O, Collepardo-Guevara R, and Schlick T, 2010. Modeling studies of chromatin fiber structure as a function of DNA linker length. Journal of Molecular Biology 403:777–802. http://www.sciencedirect.com/science/article/pii/S0022283610008338. [PubMed: 20709077]
3. Widom J, 1992. A relationship between the helical twist of DNA and the ordered positioning of nucleosomes in all eukaryotic cells. Proceedings of the National Academy of Sciences of the United States of America 89:1095–1099. [PubMed: 1736292]
4. Lohr D, and Van Holde KE, 1979. Organization of spacer DNA in chromatin. Proceedings of the National Academy of Sciences of the United States of America 76:6326–6330. https://www.pnas.org/content/76/12/6326. [PubMed: 392519]
5. Strauss F, and Prunell A, 1983. Organization of internucleosomal DNA in rat liver chromatin. The EMBO Journal 2:51–56. https://www.embopress.org/doi/abs/10.1002/j.1460-2075.1983.tb01379.x. [PubMed: 11894908]
6. Lohr D, 1986. The salt dependence of chicken and yeast chromatin structure. Effects on internucleosomal organization and relation to active chromatin. Journal of Biological Chemistry 261:9904–9914. https://www.sciencedirect.com/science/article/pii/S0021925818676021. [PubMed: 3733698]
7. Hayes JJ, Clark DJ, and Wolffe AP, 1991. Histone contributions to the structure of DNA in the nucleosome. Proceedings of the National Academy of Sciences of the United States of America 88:6829–6833. [PubMed: 1650485]
8. Hayes JJ, Tullius TD, and Wolffe AP, 1990. The structure of DNA in a nucleosome. Proceedings of the National Academy of Sciences of the United States of America 87:7405–7409. [PubMed: 2170977]
9. Wang J-P, Fondufe-Mittendorf Y, Xi L, Tsai G-F, Segal E, and Widom J, 2008. Preferentially Quantized Linker DNA Lengths in Saccharomyces cerevisiae. PLOS Computational Biology 4:1–10. 10.1371/journal.pcbi.1000175.
10. Brogaard K, Xi L, Wang JP, and Widom J, 2012. A map of nucleosome positions in yeast at base-pair resolution. Nature 486:496–501. [PubMed: 22722846]
11. Chereji RV, Ramachandran S, Bryson TD, and Henikoff S, 2018. Precise genome-wide mapping of single nucleosomes and linkers in vivo. Genome Biology 19.
12. Field Y, Kaplan N, Fondufe-Mittendorf Y, Moore IK, Sharon E, Lubling Y, Widom J, and Segal E, 2008. Distinct modes of regulation by chromatin encoded through nucleosome positioning signals. PLoS Computational Biology 4:e1000216. 10.1371/journal.pcbi.1000216. [PubMed: 18989395]

Author Manuscript Author Manuscript Author Manuscript Author Manuscript

13. Voong LN, Xi L, Sebeson AC, Xiong B, Wang JP, and Wang X, 2016. Insights into Nucleosome Organization in Mouse Embryonic Stem Cells through Chemical Mapping. Cell 167:1555–1570.e15. https://www.ncbi.nlm.nih.gov/pubmed/27889238https://www.ncbi.nlm.nih.gov/pmc/PMC5135608/. [PubMed: 27889238]

14. Cohanim AB, Kashi Y, and Trifonov EN, 2006. Three sequence rules for chromatin. Journal of Biomolecular Structure and Dynamics 23:559–566. [PubMed: 16494506]

15. Kato M, Onishi Y, Wada-Kiyama Y, Abe T, Ikemura T, Kogan S, Bolshoy A, Trifonov EN, and Kiyama R, 2003. Dinucleosome DNA of Human K562 Cells: Experimental and Computational Characterizations. Journal of Molecular Biology 332:111–125. https://www.sciencedirect.com/science/article/pii/S0022283603008386. [PubMed: 12946351]

16. Norouzi D, and Zhurkin V, 2015. Topological Polymorphism of the Two-Start Chromatin Fiber. Biophysical Journal 108:2591–2600. https://www.sciencedirect.com/science/article/pii/S000634951500394X. [PubMed: 25992737]

17. Norouzi D, Katebi A, Cui F, and Zhurkin VB, 2015. Topological diversity of chromatin fibers: Interplay between nucleosome repeat length, DNA linking number and the level of transcription. AIMS Biophysics 2:613–629. [PubMed: 28133628]

18. Nikitina T, Norouzi D, Grigoryev SA, and Zhurkin VB, 2017. DNA topology in chromatin is defined by nucleosome spacing. Science Advances 3:e1700957. https://www.science.org/doi/abs/10.1126/sciadv.1700957. [PubMed: 29098179]

19. Zhurkin VB, and Norouzi D, 2021. Topological polymorphism of nucleosome fibers and folding of chromatin. Biophysical journal 120:577–585. [PubMed: 33460599]

20. Correll SJ, Schubert MH, and Grigoryev SA, 2012. Short nucleosome repeats impose rotational modulations on chromatin fibre folding. EMBO Journal 31:2416–2426. http://www.ncbi.nlm.nih.gov/pmc/articles/PMC3364735/. [PubMed: 22473209]

21. Bass MV, Nikitina T, Norouzi D, Zhurkin VB, and Grigoryev SA, 2019. Nucleosome spacing periodically modulates nucleosome chain folding and DNA topology in circular nucleosome arrays. Journal of Biological Chemistry 294:4233–4246. [PubMed: 30630950]

22. Clauvelin N, Lo P, Kulaeva OI, Nizovtseva EV, Diaz-Montes J, Zola J, Parashar M, Studitsky VM, and Olson WK, 2015. Nucleosome positioning and composition modulate in silico chromatin flexibility. J. Phys. Condens. Matter 27:064112. https://iopscience.iop.org/article/10.1088/0953-8984/27/6/064112. [PubMed: 25564155]

23. Todolli S, Perez PJ, Clauvelin N, and Olson WK, 2017. Contributions of Sequence to the Higher-Order Structures of DNA. Biophys. J. 112:416–426. https://linkinghub.elsevier.com/retrieve/pii/S0006349516310463. [PubMed: 27955889]

24. Todolli S, Young RT, Watkins AS, Bu Sha A, Yager J, and Olson WK, 2021. Surprising Twists in Nucleosomal DNA with Implication for Higher-order Folding. J. Mol. Biol. 433:167121. https://linkinghub.elsevier.com/retrieve/pii/S0022283621003454. [PubMed: 34192585]

25. Todolli S, Nizovtseva EV, Clauvelin N, Maxian O, Studitsky VM, and Olson WK, 2024. Geometric variations in nucleosomal DNA dictate higher-order chromatin structure and enhancer–promoter communication. J. Chem. Phys. 161. https://pubs.aip.org/jcp/article/161/24/245102/3328492/Geometric-variations-in-nucleosomal-DNA-dictate.

26. Brouwer T, Pham C, Kaczmarczyk A, De Voogd WJ, Botto M, Vizjak P, Mueller-Planitz F, and Van Noort J, 2021. A critical role for linker DNA in higher-order folding of chromatin fibers. Nucleic Acids Research 49:2537–2551. [PubMed: 33589918]

27. Kenzaki H, and Takada S, 2021. Linker DNA Length is a Key to Tri-nucleosome Folding. Journal of Molecular Biology 433:166792. https://www.sciencedirect.com/science/article/pii/S0022283620307178, diving into Chromatin across Space and Time. [PubMed: 33383034]

28. Song F, Chen P, Sun D, Wang M, Dong L, Liang D, Xu RM, Zhu P, and Li G, 2014. Cryo-EM study of the chromatin fiber reveals a double helix twisted by tetranucleosomal units. Science 344:376–380. [PubMed: 24763583]

29. Schalch T, Duda S, Sargent DF, and Richmond TJ, 2005. X-ray structure of a tetranucleosome and its implications for the chromatin fibre. Nature 436:138–141. https://www.nature.com/articles/nature03686. [PubMed: 16001076]

Author Manuscript Author Manuscript Author Manuscript Author Manuscript

30. Soman A, Wong SY, Korolev N, Surya W, Lattmann S, Vogirala VK, Chen Q, Berezhnoy NV, van Noort J, Rhodes D, and Nordenskiöld L, 2022. Columnar structure of human telomeric chromatin. Nature 609:1048–1055. 10.1038/s41586-022-05236-5. [PubMed: 36104563]

31. Garcia-Saez I, Menoni H, Boopathi R, Shukla MS, Soueidan L, Noirclerc-Savoye M, Le Roy A, Skoufias DA, Bednar J, Hamiche A, Angelov D, Petosa C, and Dimitrov S, 2018. Structure of an H1-Bound 6-Nucleosome Array Reveals an Untwisted Two-Start Chromatin Fiber Conformation. Molecular Cell 72:902–915.e7. http://www.sciencedirect.com/science/article/pii/S1097276518307986. [PubMed: 30392928]

32. Dombrowski M, Engeholm M, Dienemann C, Dodonova S, and Cramer P, 2022. Histone H1 binding to nucleosome arrays depends on linker DNA length and trajectory. Nature Structural & Molecular Biology 29:493–501. 10.1038/s41594-022-00768-w.

33. Bascom GD, Myers CG, and Schlick T, 2019. Mesoscale modeling reveals formation of an epigenetically driven HOXC gene hub. Proc. Natl. Acad. Sci. 116:4955–4962. https://pnas.org/doi/full/10.1073/pnas.1816424116. [PubMed: 30718394]

34. Collepardo-Guevara R, and Schlick T, 2014. Chromatin fiber polymorphism triggered by variations of DNA linker lengths. Proceedings of the National Academy of Sciences of the United States of America 111:8061–8066. http://www.pnas.org/content/111/22/8061. [PubMed: 24847063]

35. Bascom GD, Kim T, and Schlick T, 2017. Kilobase Pair Chromatin Fiber Contacts Promoted by Living-System-Like DNA Linker Length Distributions and Nucleosome Depletion. J. Phys. Chem. B 121:3882–3894. https://pubs.acs.org/doi/10.1021/acs.jpcb.7b00998. [PubMed: 28299939]

36. Collepardo-Guevara R, and Schlick T, 2014. Chromatin fiber polymorphism triggered by variations of DNA linker lengths. Proc. Natl. Acad. Sci. 111:8061–8066. https://pnas.org/doi/full/10.1073/pnas.1315872111. [PubMed: 24847063]

37. Portillo-Ledesma S, and Schlick T, 2020. Bridging chromatin structure and function over a range of experimental spatial and temporal scales by molecular modeling. Wiley Interdisciplinary Reviews: Computational Molecular Science 10:wcms.1434.

38. Bascom GD, and Schlick T, 2017. Mesoscale Modeling of Chromatin Fibers. In Lavelle C, and Victor J-M, editors, Nuclear Architecture and Dynamics, Academic Press, Boston, volume 2, 123–147. http://www.sciencedirect.com/science/article/pii/B9780128034804000053.

39. Davey CA, Sargent DF, Luger K, Maeder AW, and Richmond TJ, 2002. Solvent Mediated Interactions in the Structure of the Nucleosome Core Particle at 1.9Å Resolution††We dedicate this paper to the memory of Max Perutz who was particularly inspirational and supportive to T.J.R. in the early stages of this study. Journal of Molecular Biology 319:1097–1113. https://www.sciencedirect.com/science/article/pii/S0022283602003868. [PubMed: 12079350]

40. Beard DA, and Schlick T, 2001. Modeling salt-mediated electrostatics of macromolecules: The discrete surface charge optimization algorithm and its application to the nucleosome. Biopolymers 58:106–115. [PubMed: 11072233]

41. Zhang Q, Beard DA, and Schlick T, 2003. Constructing Irregular Surfaces to Enclose Macromolecular Complexes for Mesoscale Modeling Using the Discrete Surface Charge Optimization (DiSCO) Algorithm. Journal of Computational Chemistry 24:2063–2074. [PubMed: 14531059]

42. Sun J, Zhang Q, and Schlick T, 2005. Electrostatic mechanism of nucleosomal array folding revealed by computer simulation. Proceedings of the National Academy of Sciences of the United States of America 102:8180–8185. https://www.ncbi.nlm.nih.gov/pubmed/15919827https://www.ncbi.nlm.nih.gov/pmc/PMC1140479/. [PubMed: 15919827]

43. Arya G, Zhang Q, and Schlick T, 2006. Flexible histone tails in a new mesoscopic oligonucleosome model. Biophysical Journal 91:133–150. [PubMed: 16603492]

44. Luque A, Collepardo-Guevara R, Grigoryev S, and Schlick T, 2014. Dynamic condensation of linker histone C-terminal domain regulates chromatin structure. Nucleic Acids Research 42:7553–7560. [PubMed: 24906881]

45. Jian H, Vologodskii AV, and Schlick T, 1997. A combined wormlike-chain and bead model for dynamic simulations of long linear DNA. Journal of Computational Physics 136:168–179. http://www.sciencedirect.com/science/article/pii/S002199919795765X.

Author Manuscript Author Manuscript Author Manuscript Author Manuscript

46. Horowitz DS, and Wang JC, 1984. Torsional rigidity of DNA and length dependence of the free energy of DNA supercoiling. Journal of Molecular Biology 173:75–91. https://www.sciencedirect.com/science/article/pii/0022283684904042. [PubMed: 6321743]
47. Stigter D, 1977. Interactions of highly charged colloidal cylinders with applications to double-stranded DNA. Biopolymers 16:1435–1448. https://onlinelibrary.wiley.com/doi/10.1002/bip.1977.360160705. [PubMed: 880366]
48. Arya G, and Schlick T, 2007. Efficient global biopolymer sampling with end-transfer configurational bias Monte Carlo. Journal of Chemical Physics 126:44107.
49. Metropolis N, and Ulam S, 1949. The Monte Carlo Method. Journal of the American Statistical Association 44:335–341. https://www.tandfonline.com/doi/abs/10.1080/01621459.1949.10483310. [PubMed: 18139350]
50. Rosenbluth MN, and Rosenbluth AW, 1955. Monte Carlo calculation of the average extension of molecular chains. J. Chem. Phys. 23:356–359. 10.1063/1.1741967.
51. Drew HR, and Travers AA, 1985. DNA bending and its relation to nucleosome positioning. Journal of Molecular Biology 186:773–790. [PubMed: 3912515]
52. Garcia-Ramirez M, Dong F, and Ausio J, 1992. Role of the histone “tails” in the folding of oligonucleosomes depleted of histone H1. The Journal of biological chemistry 267:19587–19595. [PubMed: 1527076]
53. Butler P, 1998. Dinucleosomes show compaction by ionic strength, consistent with bending of linker DNA. Journal of Molecular Biology 281:401–407. [PubMed: 9698556]
54. Perišić O, Collepardo-Guevara R, and Schlick T, 2010. Modeling studies of chromatin fiber structure as a function of DNA linker length. Journal of Molecular Biology 403:777–802. [PubMed: 20709077]
55. Routh A, Sandin S, and Rhodes D, 2008. Nucleosome repeat length and linker histone stoichiometry determine chromatin fiber structure. Proceedings of the National Academy of Sciences 105:8872–8877. https://www.pnas.org/doi/abs/10.1073/pnas.0802336105.
56. Nizovtseva EV, Todolli S, Olson WK, and Studitsky VM, 2017. Towards Quantitative Analysis of Gene Regulation by Enhancers. Epigenomics 9:1219–1231. https://www.tandfonline.com/doi/full/10.2217/epi-2017-0061. [PubMed: 28799793]
57. Happel N, and Doenecke D, 2009. Histone H1 and its isoforms: Contribution to chromatin structure and function. Gene 431:1–12. https://linkinghub.elsevier.com/retrieve/pii/S0378111908005684. [PubMed: 19059319]
58. Luque A, Ozer G, and Schlick T, 2016. Correlation among DNA Linker Length, Linker Histone Concentration, and Histone Tails in Chromatin. Biophys J 110:2309–2319. [PubMed: 27276249]
59. Allahverdi A, Chen Q, Korolev N, and Nordenskiöld L, 2015. Chromatin compaction under mixed salt conditions: Opposite effects of sodium and potassium ions on nucleosome array folding. Sci. Rep. 5:8512. https://www.nature.com/articles/srep08512. [PubMed: 25688036]
60. Korolev N, 2021. How potassium came to be the dominant biological cation: of metabolism, chemiosmosis, and cation selectivity since the beginnings of life. BioEssays 43. https://onlinelibrary.wiley.com/doi/10.1002/bies.202000108.
61. Grigoryev SA, Bascom G, Buckwalter JM, Schubert MB, Woodcock CL, and Schlick T, 2016. Hierarchical looping of zigzag nucleosome chains in metaphase chromosomes. Proc. Natl. Acad. Sci. 113:1238–1243. https://pnas.org/doi/full/10.1073/pnas.1518280113. [PubMed: 26787893]
62. Jentink N, Purnell C, Kable B, Swulius MT, and Grigoryev SA, 2023. Cryoelectron tomography reveals the multiplex anatomy of condensed native chromatin and its unfolding by histone citrullination. Mol. Cell 83:3236–3252.e7. https://linkinghub.elsevier.com/retrieve/pii/S1097276523006536. [PubMed: 37683647]
63. Gómez-García PA, Portillo-Ledesma S, Neguembor MV, Pesaresi M, Oweis W, Rohrlich T, Wieser S, Meshorer E, Schlick T, Cosma MP, and Lakadamyali M, 2021. Mesoscale Modeling and Single-Nucleosome Tracking Reveal Remodeling of Clutch Folding and Dynamics in Stem Cell Differentiation. Cell Reports 34:108614. https://www.sciencedirect.com/science/article/pii/S221112472031603X. [PubMed: 33440158]
64. Portillo-Ledesma S, Hang M, and Schlick T, 2025. Regulation of chromatin architecture in Huntington’s disease. Biochemistry.

Author Manuscript Author Manuscript Author Manuscript Author Manuscript

65. Arya G, and Schlick T, 2009. A Tale of Tails: How Histone Tails Mediate Chromatin Compaction in Different Salt and Linker Histone Environments. J. Phys. Chem. A 113:4045–4059. https://pubs.acs.org/doi/10.1021/jp810375d. [PubMed: 19298048]

66. Li Z, Portillo-Ledesma S, Janani M, and Schlick T, 2025. Incorporating multiscale methylation effects into nucleosome-resolution chromatin models for simulating mesoscale fibers. J. Chem. Phys. 162. https://pubs.aip.org/jcp/article/162/9/094107/3338760/Incorporating-multiscale-methylation-effects-into.

67. Kable B, Portillo-Ledesma S, Popova EY, Jentink N, Swulius M, Li Z, Schlick T, and Grigoryev SA, 2025. Compromised 2-start zigzag chromatin folding in immature mouse retina cells driven by irregularly spaced nucleosomes with short DNA linkers. bioRxiv https://www.biorxiv.org/content/early/2025/01/16/2025.01.16.633430.

68. Lohr D, Corden J, Tatchell K, Kovacic RT, and Van Holde KE, 1977. Comparative subunit structure of HeLa, yeast, and chicken erythrocyte chromatin. Proc. Natl. Acad. Sci. 74:79–83. https://pnas.org/doi/full/10.1073/pnas.74.1.79. [PubMed: 319461]

69. Makarov VL, Lejnine S, Bedoyan J, and Langmore JP, 1993. Nucleosomal organization of telomere-specific chromatin in rat. Cell 73:775–787. https://www.sciencedirect.com/science/article/pii/009286749390256P. [PubMed: 8500170]

70. Thomas JO, and Thompson R, 1977. Variation in chromatin structure in two cell types from the same tissue: a short DNA repeat length in cerebral cortex neurons. Cell 10:633–640. https://www.sciencedirect.com/science/article/pii/0092867477900964. [PubMed: 862024]

71. Wang J-P, Fondufe-Mittendorf Y, Xi L, Tsai G-F, Segal E, and Widom J, 2008. Preferentially Quantized Linker DNA Lengths in Saccharomyces cerevisiae. PLoS Comput. Biol. 4:e1000175. https://dx.plos.org/10.1371/journal.pcbi.1000175. [PubMed: 18787693]

72. Lieberman-Aiden E, van Berkum NL, Williams L, Imakaev M, Ragoczy T, Telling A, Amit I, Lajoie BR, Sabo PJ, Dorschner MO, Sandstrom R, Bernstein B, Bender MA, Groudine M, Gnirke A, Stamatoyannopoulos J, Mirny LA, Lander ES, and Dekker J, 2009. Comprehensive Mapping of Long-Range Interactions Reveals Folding Principles of the Human Genome. Science (80-.). 326:289–293. https://www.science.org/doi/10.1126/science.1181369.

Author Manuscript Author Manuscript Author Manuscript Author Manuscript

SIGNIFICANCE

This study provides new insights into how linker DNA periodicities ($10n$ and $10n + 5$) influence chromatin architecture at high resolution. Using a refined mesoscale chromatin model, we reveal that periodicity-driven effects significantly affect fiber compaction in zigzag topologies at short linker length values, and that these effects are likely absent in longer linkers and solenoid fibers. The results also emphasize the role of linker histones, salt concentration, fiber topology design, and heterogeneous linker DNAs in modulating chromatin topologies. By connecting nucleosome spacing to chromatin topology and flexibility, this work advances our understanding of chromatin dynamics and its implications for gene regulation, offering valuable perspectives for both experimental and computational research in chromatin biology.

Author Manuscript Author Manuscript Author Manuscript Author Manuscript

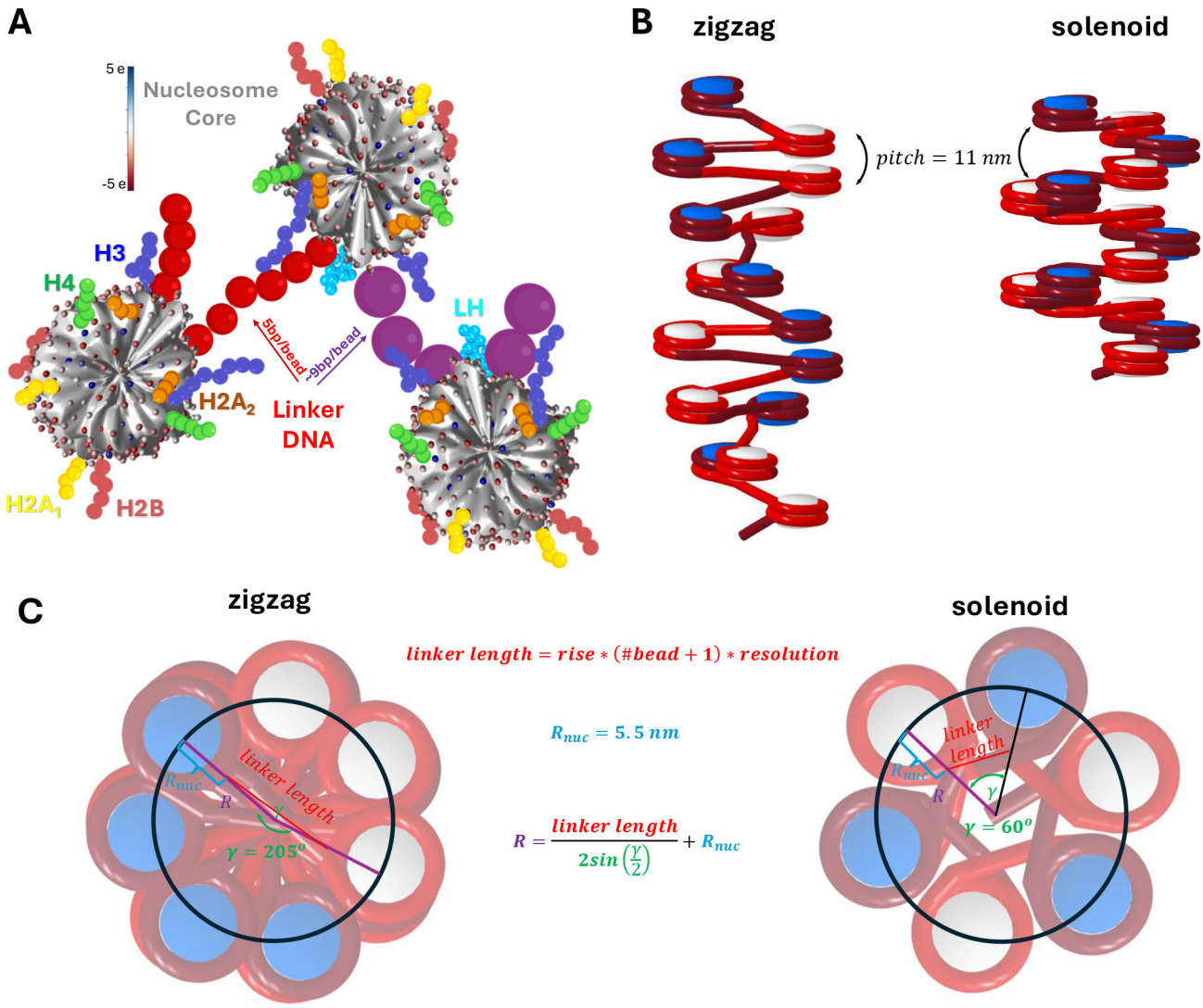


Figure 1: Mesoscale Chromatin Model.

A. Model constituents include: nucleosome cores with 300 charged beads, linker DNA beads of 5 bp/bead (red) or ~9 bp/bead (purple) resolution, histone N-terminal tails of H2A (yellow), H2B (dark pink), H3 (blue), and H4 (green), C-terminal tail of H2A (orange), and LHs (cyan). B. Initial conformations of ideal zigzag and solenoid chromatin fibers: side view of zigzag (left) and solenoid (right) fibers; both have a pitch of 11 nm, but zigzag has roughly 2 nucleosomes per turn, and solenoid has 6 nucleosomes per turn. C. Top view of the zigzag (left) and solenoid (right) fibers and the details of calculating helix radius (R) based on linker length, angle per core (γ), and nucleosome radius.

Author Manuscript Author Manuscript Author Manuscript Author Manuscript

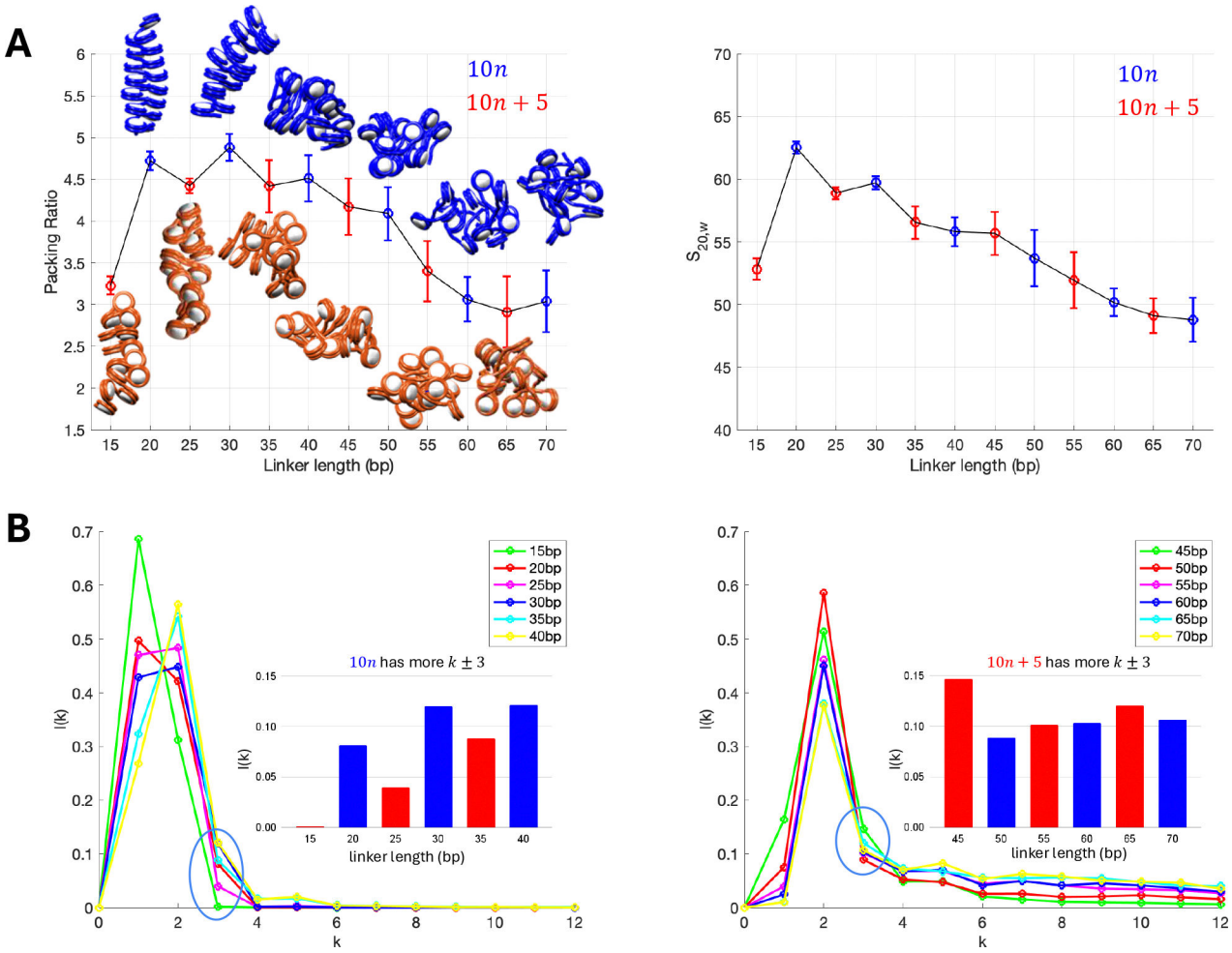


Figure 2: Compaction and interaction trends for 16-nucleosome fibers with $10n$ vs. $10n + 5$ linker DNA lengths (without linker histone) at the monovalent salt concentration of 150 mM started from zigzag fiber.

A. Packing ratio (left) and sedimentation (right) profiles for chromatin fibers with linker lengths ranging from 15 to 70 bp. B. Core-core interaction frequencies, shown separately for 15–40 bp (left) and 45–70 bp (right) fibers. Insets show $k \pm 3$ interactions as a function of linker DNA length.

Author Manuscript Author Manuscript Author Manuscript Author Manuscript

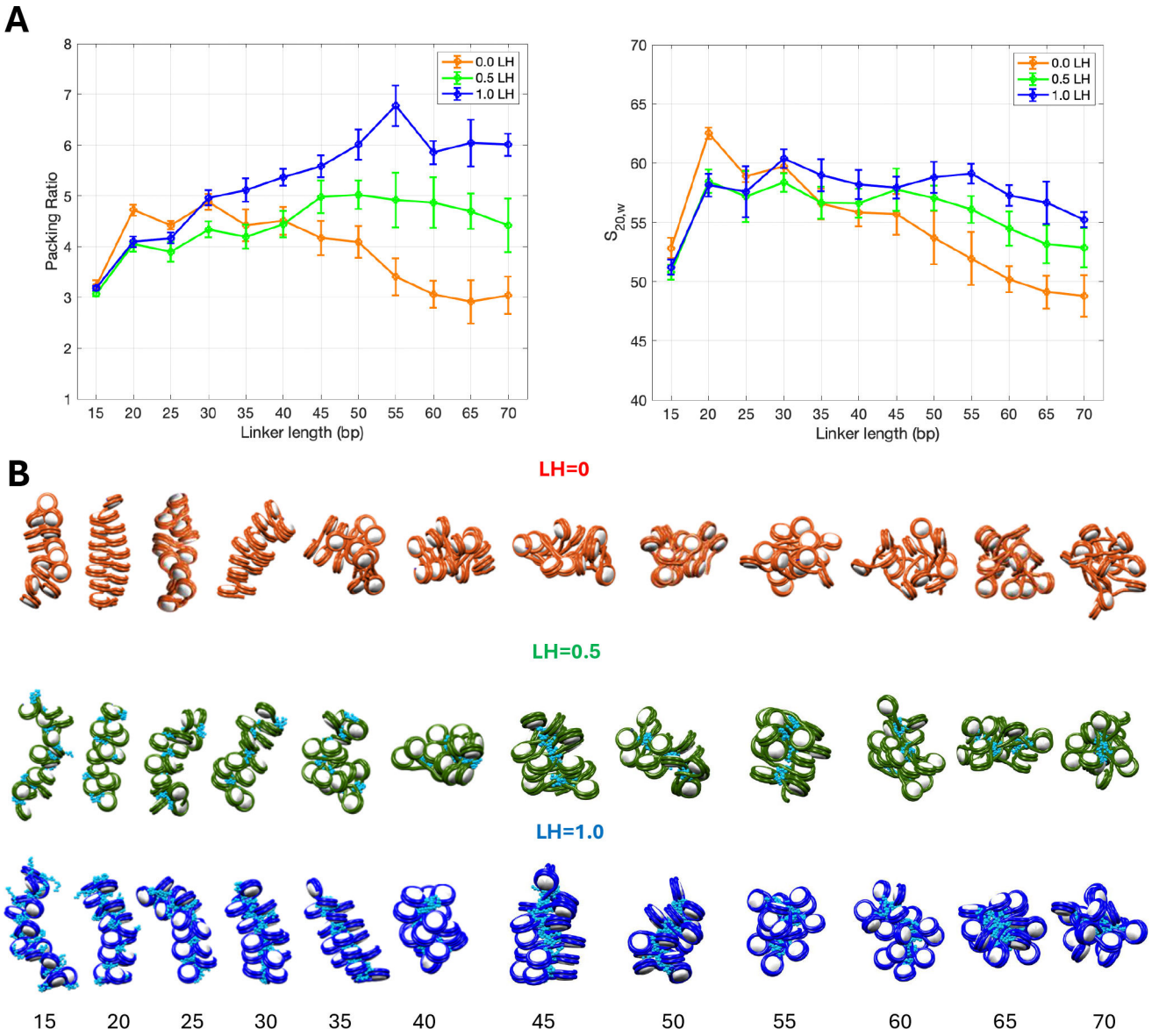


Figure 3: Compaction trends of $10n$ vs. $10n + 5$ linker DNA for 16-nucleosome fibers at increasing LH density at 150 mM salt concentration from zigzag start topology.

A. Packing ratio (left) and sedimentation (right) for fibers with linker DNA lengths of 15 to 70 bp and with different LH densities: 0, 0.5, and 1 LH per nucleosome. B. Representative fiber structures in each condition with LHs shown in turquoise.

Author Manuscript Author Manuscript Author Manuscript Author Manuscript

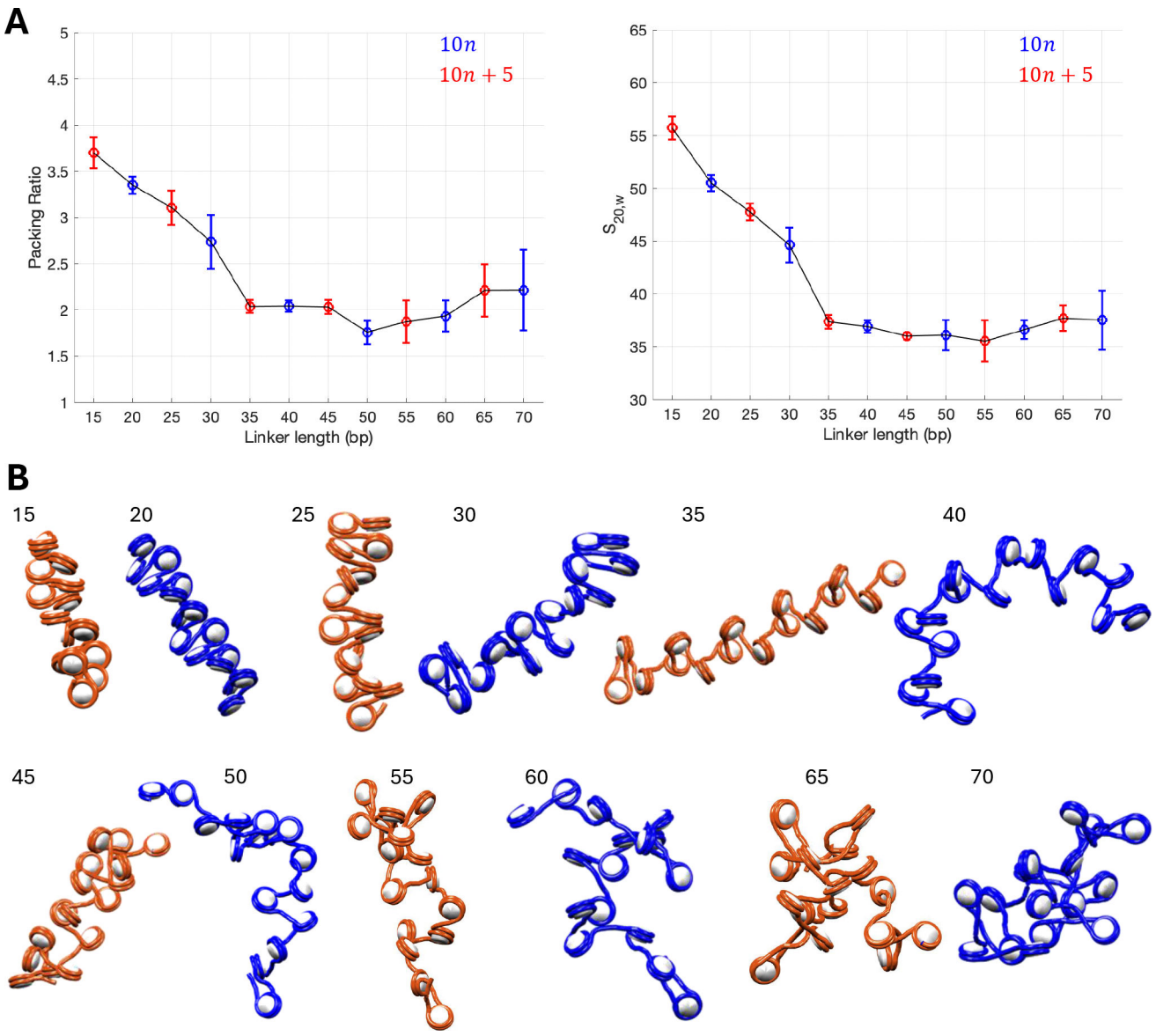


Figure 4: Effect of low salt concentration on compaction trends of $10n$ vs. $10n + 5$ linker DNA for 16-nucleosome fibers, without linker histones from zigzag starting topology.

A. Packing ratio (left) and sedimentation (right) for fibers with linker DNA lengths of 15 to 70 bp at 5 mM NaCl. B. Representative fiber structures in each condition.

Author Manuscript Author Manuscript Author Manuscript Author Manuscript

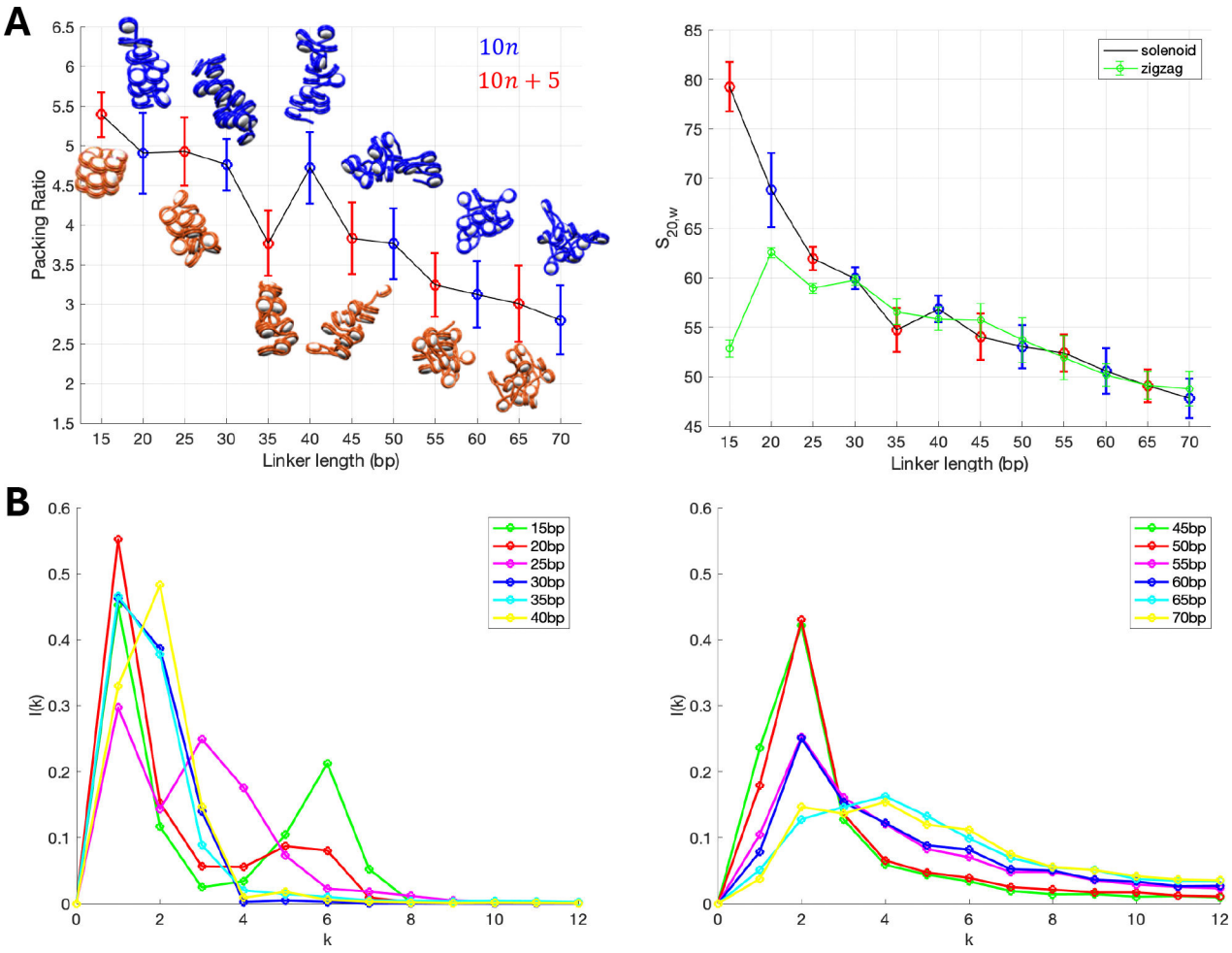


Figure 5: Compaction trends of $10n$ vs. $10n + 5$ linker DNA for 16-nucleosome fibers without linker histone at 150 mM salt starting from solenoid topologies.

A. Packing ratio (left) and sedimentation (right) for fibers with linker lengths of 15 to 70 bp. B. Core-core interaction frequencies, shown separately for 15–40 bp (left) and 45–70 bp (right) fibers.

Author Manuscript Author Manuscript Author Manuscript Author Manuscript

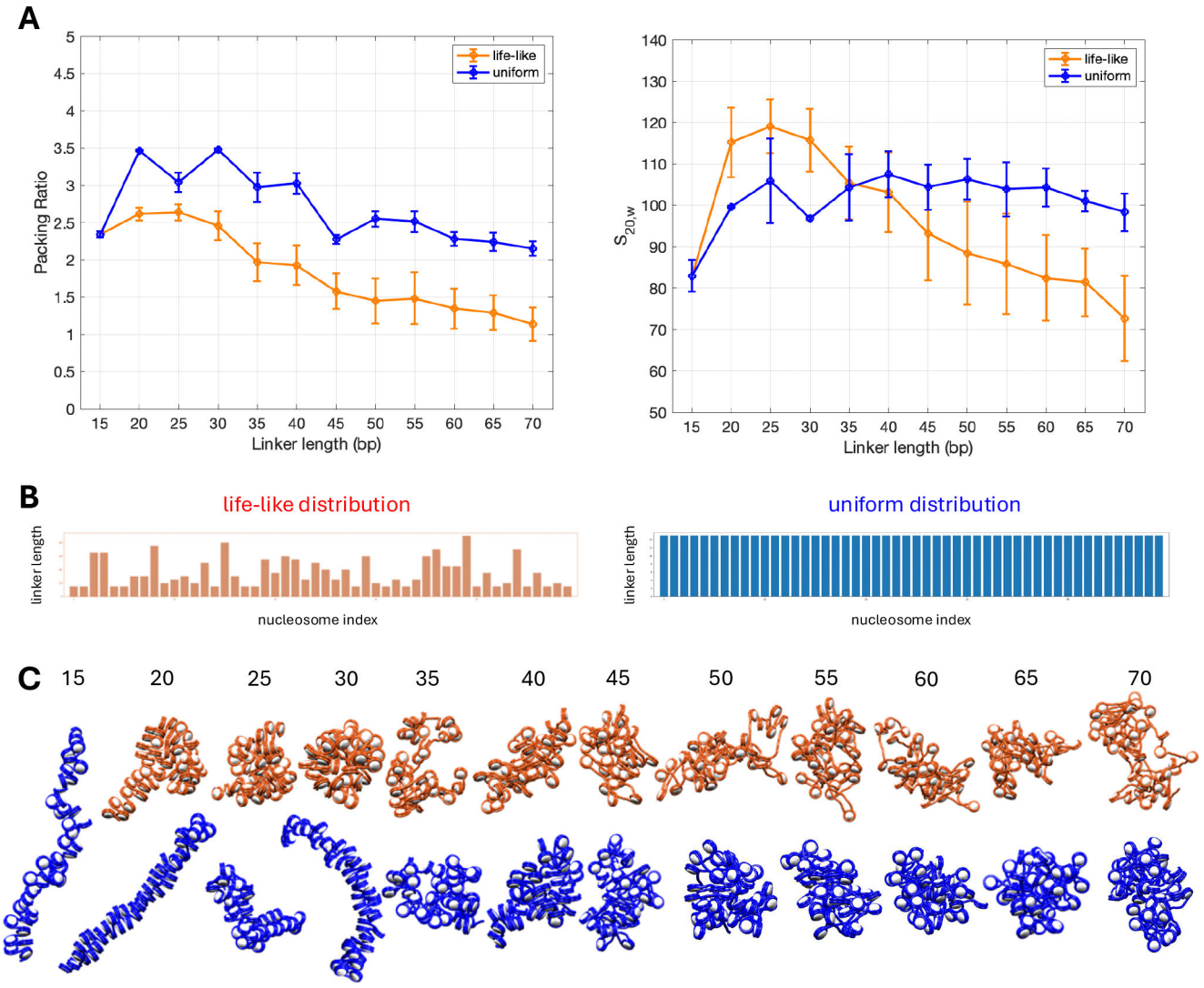


Figure 6: Effect of mixture of irregular linker DNA lengths on compaction trends of $10n$ vs. $10n + 5$ linker DNA for 50-nucleosome fibers without linker histone, at 150 mM salt starting from zigzag topology.

A. Packing ratio (left) and sedimentation (right) for fibers with linker lengths of 15 to 70 bp obtained by uniform (blue) or life-like (orange) distributions. B. Representative linker length distributions for life-like (left) and uniform (right) systems; C. Representative structures for chromatin fibers with irregular (orange) and uniform (blue) linker lengths.

Author Manuscript Author Manuscript Author Manuscript Author Manuscript

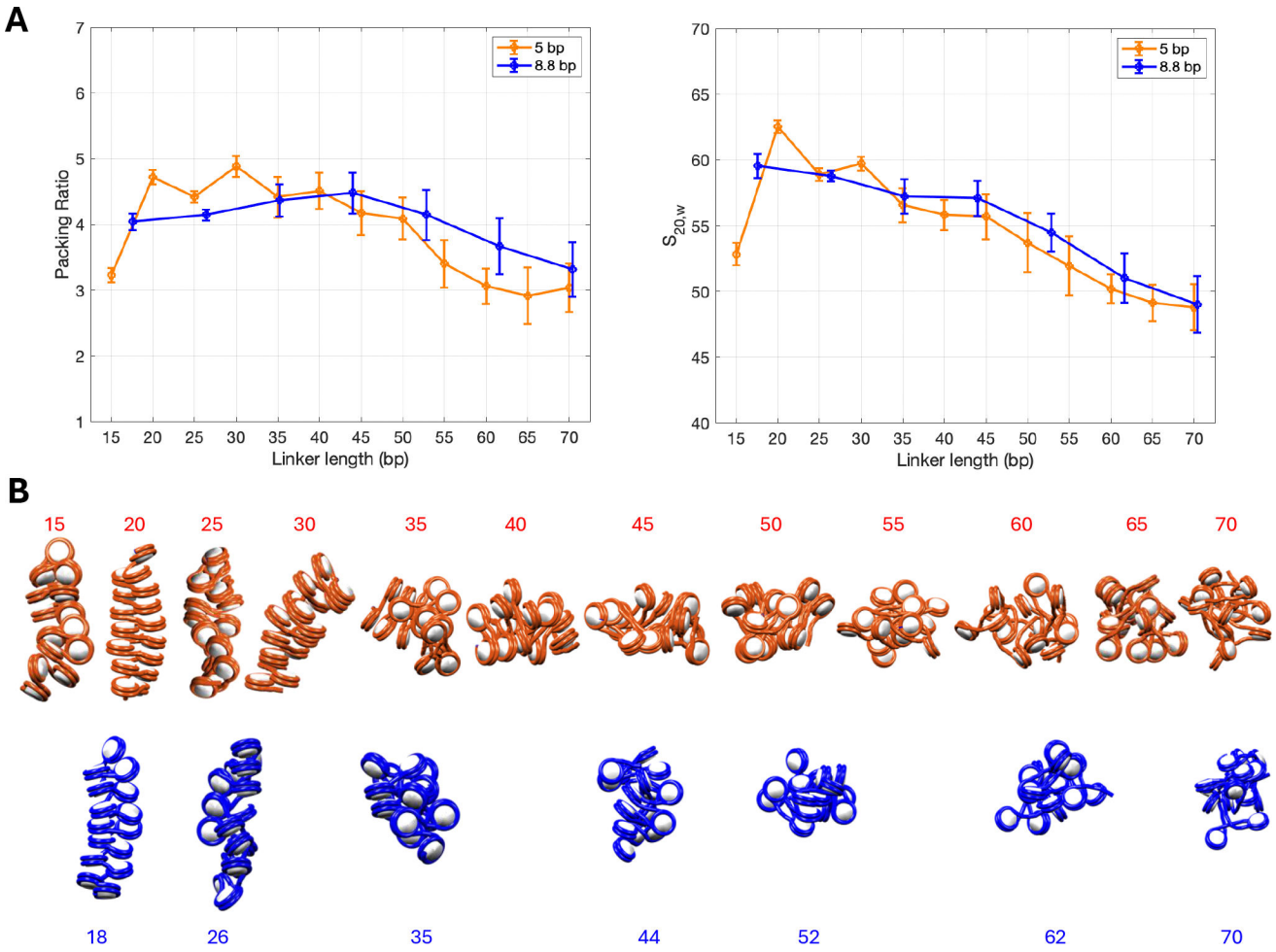


Figure 7: Effect of linker DNA resolution model.

Compaction trends (A) and configurations (B) for 16-nucleosome fibers with linker lengths of 15 to 70 bp obtained with our former ~9 bp DNA resolution model (blue) and the new 5 bp model (orange), at 150 mM salt, without linker histone, started from zigzag topology.

Author Manuscript Author Manuscript Author Manuscript Author Manuscript

Table 1:

Summary of simulation studies comparing $10n$ and $10n + 5$ linker spacing.

Group/Ref.	Start Topology	System	Salt	Findings
Zhurkin (16)	2-start	12 nucleosomes	implicit	$10n$ linkers lead to stable, compact, and stacked fibers. $10n + 5$ linkers result in more flexible, less stable fibers with weaker stacking and different DNA supercoiling.
Zhurkin (17)	2-start	16 nucleosomes	implicit	$10n$ linkers produce compact and stable fibers with ΔLk ≈ -1.5. $10n + 5$ linkers produce more flexible and less stable fibers, with ΔLk ≈ -1.0.
Grigoryev and Zhurkin (21)	2/3-start	12 nucleosomes	implicit	At 150 mM NaCl, $10n$ arrays are more compact and have stronger $i = 2$ internucleosome interactions, while $10n + 5$ arrays are more flexible and show stronger $i = 3$ interactions. $10n$ arrays introduce more negative supercoils than $10n + 5$.
Zhurkin (19)	2-start	12 nucleosomes	implicit	Fibers with $10n$ linker spacing form more compact and supercoiled structures, while $10n + 5$ spacing leads to more flexible conformations. This topological polymorphism may underlie functional chromatin differences.
van Noort (26)	0/1/2-start	16 nucleosomes	implicit	10 bp periodic modulation appears in folding energy and stiffness. $10n$ linkers favor optimal stacking; $10n + 5$ spacing disrupts folding, especially when NRL is short.
Olson (22, 23)	2/3-start	13 and 20 nucleosomes, 1kx5	implicit	Understwisted nucleosomal DNA (1kx5) and $10n$-like spacing favors long, flexible, 3-start arrays, while $10n + 5$ leads to stiffer, shorter, 2-start fibers.
Olson (24, 25)	2/3-start	4–13 nucleosomes, 1kx5 and 5b0z	implicit	Nucleosomal DNA twist affects fiber topology. Overtwisted nucleosomal DNA (5b0z) favors 2-start topologies for $10n$ linkers and 3-start topologies for $10n + 5$ linkers.
Takada (27)	3-start	3 nucleosomes	implicit, 150 mM monovalent ion	$10n$ linkers produce compact zigzag fibers, $10n + 5$ leads to more variable conformations.
This work	1/2-start	16 and 50 nucleosomes	implicit, 5 and 150 mMNaCl	$10n$ linkers with zigzag start produce more compact structures than $10n + 5$ linkers. This applies to short linker lengths, NaCl 150 mM, and LH density ≤0.5. Periodicity is lost for lower monovalent salt, high LH densities, solenoid start, and “life-like” fibers.

Author Manuscript

Author Manuscript

Author Manuscript

Author Manuscript

Table 2:

Linker DNA length and NRL across different organisms

Organism	Linker Length Range (bp)	Nucleosome Repeat Length (bp)	Notes
Yeast (Saccharomyces cere-visiae, Schizosaccharomyces pombe) (71)	5–45	168 ± 14	Linker DNA follows a $10n + 5$ bp periodicity
Human (K562 cells) (62)	38–60	188 ± 18	NRL suggest that linker DNA follows a periodic pattern, although local chromatin states (e.g., euchromatin vs. heterochromatin) affect spacing.
Human (HeLa cells) (21, 61, 68)	36–41	185 ± 3	Chromatin maintains zigzag folding in both interphase and metaphase; linker histone modulates hierarchical looping
Chicken (Gallus gallus, erythrocytes) (61, 68)	58	197	Nucleosome organization follows phased patterns but does not exhibit $10n + 5$ periodicity; supports a stable 30-nm fiber with two-start zigzag geometry
Mouse (embryonic stem cells) (13)	20–60	190 ± 23	Linker DNA follows a $10n + 5$ bp periodicity
Rat (Liver, telomers) (69)	10	157 ± 2	Very short linker DNA
Rabbit (Cerebral Cortex Neurons) (70)	9–25	164±8	Cerebral cortex neurons have a significantly shorter repeat length and linker DNA compared to other cell types in the same tissue